Analysis of infrared spectra of gaseous TlF

J.F. OGILVIE[1] AND S.C. LIAO
Academia Sinica, Institute of Atomic and Molecular Sciences, P.O. Box 23-166, Taipei 10764, Taiwan

AND

HIROMICHI UEHARA AND KOUI HORIAI
Department of Chemistry, Faculty of Science, Josai University, Keyakidai, Sakado, Saitama 350-02, Japan

Received March 10, 1994
Accepted June 27, 1994

This paper is dedicated to Dr. Gerhard Herzberg on the occasion of his 90th birthday

Vibration–rotational spectra of $^{205}Tl^{19}F$ and $^{203}Tl^{19}F$ in the electronic ground state $X0^+$ were measured in absorption in the range of wave number $44\,900 \leq \tilde{\nu}/m^{-1} \leq 50\,000$ with diode lasers as spectral sources. Analysis of all available data yielded values of coefficients of radial functions for the potential energy and other molecular properties; only eight independently fitted and two constrained parameters sufficed to reproduce satisfactorily and with physical meaning the frequencies and wave numbers of about 890 distinct pure rotational and vibration–rotational transitions. Independent of nuclear mass, the equilibrium internuclear separation R_e of TlF is $(2.084\ 3517 \pm 0.000\ 0039) \times 10^{-10}$ m; the maximum range of validity of radial functions is $1.85 \leq R/10^{-10}\,m \leq 2.45$. Comparing these results with those of InF, we attribute the large magnitude of u_1^{Tl} to the finite and isotopically varying nuclear volume of Tl rather than to (adiabatic) effects of nuclear mass, whereas no such effect is detectable for In in InF. Other aspects of nonadiabatic effects for these polar molecules TlF and InF are discussed.

Les spectres de vibration–rotation de $^{205}Tl^{19}F$ et $^{203}Tl^{19}F$ dans l'état électronique fondamental $X0^+$ ont été mesurés en absorption dans l'intervalle de nombre d'onde $44\,900 \leq \tilde{\nu}/m^{-1} \leq 50\,000$ avec des lasers diodes comme sources spectrales. L'analyse de toutes les données disponibles a donné des valeurs des coefficients des fonctions radiales pour l'énergie potentielle et d'autres propriétés moléculaires. Il suffit de seulement huit paramètres ajustés indépendamment et de deux paramètres fixés pour reproduire de façon satisfaisante et physiquement significative les fréquences et les nombres d'onde d'environ 890 transitions de rotation pure ou de vibration–rotation. La séparation internucléaire à l'équilibre de TlF, indépendante de la masse nucléaire, est $(2{,}084\ 3517 \pm 0{,}000\ 0039) \times 10^{-10}$ m; l'intervalle maximum de validité des fonctions radiales est $1{,}85 \leq R/10^{-10}\,m \leq 2{,}45$. Comparant ces résultats avec ceux de InF, nous attribuons la grande valeur de u_1^{Tl} à la valeur finie et isotopiquement variable du volume nucléaire de Tl plutôt qu'à des effets (adiabatiques) de la masse nucléaire, vu qu'aucun effet de la sorte n'est détectable pour In dans InF. D'autres aspects des effets non adiabatiques pour ces molécules polaires TlF et InF sont discutés.

[Traduit par la rédaction]

Can. J. Phys. **72**, 930 (1994)

1. Introduction

During the past half century the range of gaseous molecular species amenable to investigation by means of their vibration–rotational spectra has greatly expanded. For instance, according to the compilation of diatomic molecules in Herzberg's monograph in 1950 [1], infrared and Raman spectra of only several free molecules, such as hydrogen halides, CO, NO, N_2, and O_2, had been recorded directly, although vibrational and rotational properties of many others had been characterized indirectly by means of their electronic spectra. After implementation of first microwave spectroscopy and later both interferometric techniques, for emission and absorption spectra, and laser diodes as tunable sources for absorption in the infrared region, both the range of species detected and the quality of their molecular parameters greatly increased.

The molecular species TlF provides an instance of this trend. Although pure TlF exists normally as an ionic crystalline compound at 300 K, the vapours above various solid materials containing Tl and F at temperatures 700–1200 K consist in part of discrete diatomic molecules TlF. According to this property their microwave transitions were first detected in 1958 [2], and later investigations by means of Stark and Zeeman effects [3–7] yielded further information on rotational, electric, and magnetic properties of the free molecules. Emission spectra are readily measured interferometrically; our previous experiments [8] at an effective resolution 10 m^{-1} enabled assignment of 760 lines in the sequence $\Delta v = 1$, 576 lines of $^{205}Tl^{19}F$ with $0 \leq v \leq 5$, and 184 lines of $^{203}Tl^{19}F$ with $0 \leq v \leq 3$, in the range $38\,000 \leq \tilde{\nu}/m^{-1} \leq 50\,000$. In the present work with diode lasers as sources appropriate to measure lines of Doppler width 0.07 m^{-1} at 900 K, we measured absorption of TlF in the range $44\,900 \leq \tilde{\nu}/m^{-1} \leq 50\,000$; these measurements enable significantly improved definition of molecular parameters based on the systematic theoretical treatment [9] of adiabatic, nonadiabatic, and other effects. We evaluated, accordingly, the coefficients in applicable radial functions and other molecular properties that are independent of mass, to the extent limited by the quality and quantity of all pertinent spectral data, and compare here the results with those for InF. We previously demonstrated that for AlF, for which no data on isotopic variants exist, only eight independent parameters, all related to only the (adiabatic) potential-energy function, sufficed [10] to reproduce 30 pure rotational transitions up to $v = 4$ and $J = 11$ and 519 vibration–rotational transitions up to $v = 5$ and $J = 91$. An aspect of interest in the present work is the nature of detectable effects other than potential energy that influence the measured frequencies of transitions. The adiabatic effects for Tl, which imply dependence on isotopic mass, are found to be less important than the effect of finite and isotopically varying volume.

[1]Author to whom correspondence may be addressed.

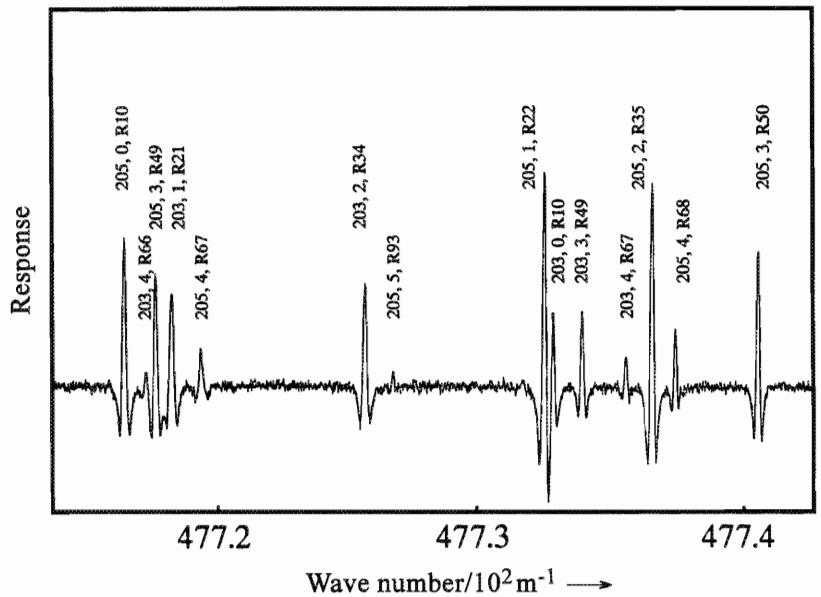

FIG. 1. Portion of the infrared absorption spectrum of TlF vapour in the region $47\,710 < \tilde{\nu}/\mathrm{m}^{-1} < 47\,750$; the ordinate represents the second derivative of the absorption in arbitrary units; the characters above each line indicate in turn the isotopic variant (203 for $^{203}Tl^{19}F$ and 205 for $^{205}Tl^{19}F$), the quantum number v of the vibrational state of smaller energy (in the sequence with $\Delta v = 1$), and the quantum number J of the rotational state in vibrational state v from which the transition occurred in absorption in the R branch.

2. Experiments

A single-pass cell was incorporated into the optical system of a spectrometer (Spectra Physics, Laser Photonics SP5000) with a diode laser as source. This heat-pipe cell consisted of a tube of stainless steel of inner diameter 30 mm and length 0.80 m; the inner wall of this tube was lined with a mesh wick also of stainless steel. The central zone of this tube, of length 0.1 m, was heated with an electric furnace. Both ends of the cell were sealed with thallium bromoiodide (KRS-5) windows that were maintained near ambient temperature by means of water cooling of the end portions of the cell.

Charging the cell with a mixture consisting of TlF (10 g), Tl (4 g), and AlF_3 (7 g) and heating the cell to ~925 K, we generated gaseous TlF in the presence of other species. A buffer gas, argon (at a pressure 800 Pa), suppressed migration of sample gas from the heated zone of the cell.

The spectrometer was equipped with two photoconductive detectors, copper-doped germanium (Ge:Cu) cooled with liquid helium. An etalon of cadmium telluride (CdTe) with an air space and a free spectral range 3.00 m^{-1} was used to measure the difference between the wavelengths of the calibration line and a line of TlF. When modulation at 1 kHz was applied to the laser source, the resulting absorption signal was 2f-detected with a phase-sensitive detector; the recorded signal exhibited the second derivative of the line shape.

The wave numbers of the spectral lines of TlF were calibrated with the spectrum of SO_2 (J.W.C. Johns, private communication), which provides reference lines with an absolute accuracy 0.02 m^{-1}. The procedure of measurement consisted of four successive scans in each set, namely of TlF, TlF plus SO_2, SO_2, and etalon. Most lines of TlF were well calibrated; in these cases we expect the errors of measurement to be less than 0.1 m^{-1}, consistent with the linewidth due to collisional broadening, about 0.2 m^{-1} under typical experimental conditions.

Using two laser diodes, we measured spectral lines of TlF in the range $44\,900 \leq \tilde{\nu}/\mathrm{m}^{-1} \leq 50\,000$. In total, 230 vibration–rotational lines were assigned to bands in the sequence with $\Delta v = 1$, 121 lines to bands with vibrational quantum numbers 1–0 to 8–7 of $^{205}Tl^{19}F$ including lines involving rotational states to $J = 148$, and 109 lines in the sequence 1–0 to 7–6 of $^{203}Tl^{19}F$ and states to $J = 143$, including 19 lines in P branches, 211 lines in R branches, and some lines of both species beyond band heads; the wave numbers of these lines appear in Tables 1 and 2, respectively. A portion of the observed spectrum is illustrated in Fig. 1.

3. Theoretical basis of spectral analysis

As the basis of a quantitative treatment we adopted an effective Hamiltonian for nuclear motion of the form [11]

$$\mathcal{H}_{\mathrm{eff}} = \hat{P}[1 + \beta(R)]\frac{\hat{P}}{2\mu} + V(R) + V'(R) + hcB_e[1 + \alpha(R)]J(J+1)\frac{R_e^2}{R^2} \quad (1)$$

Here R is the internuclear separation and R_e its value at the minimum of potential energy, μ is the reduced mass, $B_e \equiv h/(8\pi^2 c\mu R_e^2)$ is the equilibrium rotational parameter, and $\hat{P}$ is the operator for linear momentum of the nuclei. To apply this Hamiltonian we transformed to the reduced displacement variable

$$z \equiv \frac{2(R - R_e)}{(R + R_e)} \quad (2)$$

which remains finite throughout the range of molecular existence: for $0 \leq R < \infty$, $-2 \leq z < 2$ [12, 13]. With SI units of wave number [14], we represent the potential energy $V(R)$ formally independent of nuclear mass in the form [12]

TABLE 1. Assignments of vibration–rotational transitions of $^{205}Tl^{19}F$ measured with a diode laser[a]

$^{205}Tl^{19}F$ $v' = 1 \leftarrow v'' = 0$					
Line	$\tilde{\nu}/m^{-1}$	$\delta\tilde{\nu}/m^{-1}$	Line	$\tilde{\nu}/m^{-1}$	$\delta\tilde{\nu}/m^{-1}$
P (43)	45 070.36	0.03	*R* (63)	49 450.37	−0.05
P (37)	45 405.91	−0.03	*R* (64)	49 474.46	0
R (9)	47 675.52	0.08	*R* (65)	49 498.17	0.01
R (10)	47 716.56	−0.04	*R* (66)	49 521.56	0.02
R (16)	47 957.16	0.02	*R* (67)	49 544.58	0
R (19)	48 073.22	−0.05	*R* (78)	49 776.02	−0.04
R (20)	48 111.30	−0.06	*R* (79)	49 795.05	−0.05
R (21)	48 149.31*	0.17	*R* (80)	49 813.81	0.02
R (25)	48 297.17	0	*R* (81)	49 832.15	0
R (32)	48 544.19	−0.01	*R* (82)	49 850.19	0.02
R (45)	48 961.95	0.06	*R* (83)	49 867.89	0.04
R (49)	49 079.21*	−0.33	*R* (84)	49 885.19	0
R (50)	49 108.09	−0.06	*R* (85)	49 902.24	0.04
R (51)	49 136.47	0.04			

$^{205}Tl^{19}F$ $v' = 2 \leftarrow v'' = 1$					
Line	$\tilde{\nu}/m^{-1}$	$\delta\tilde{\nu}/m^{-1}$	Line	$\tilde{\nu}/m^{-1}$	$\delta\tilde{\nu}/m^{-1}$
P (38)	44 919.00	−0.06	*R* (92)	49 545.45	0.02
P (36)	45 028.56	0.01	*R* (93)	49 559.68*	0.17
P (29)	45 402.81	−0.07	*R* (113)	49 768.67	0.03
R (20)	47 661.46	0.01	*R* (114)	49 775.44	0.01
R (21)	47 698.94	−0.02	*R* (115)	49 781.84	−0.02
R (22)	47 736.27	0.10	*R* (116)	49 787.93	−0.01
R (28)	47 952.89	0.02	*R* (117)	49 793.62	−0.05
R (32)	48 091.14	0.03	*R* (118)	49 798.99	−0.05
R (33)	48 124.91	0.03	*R* (119)	49 803.98	−0.08
R (38)	48 289.16	0.12	*R* (120)	49 808.66	−0.06
R (43)	48 445.29	0	*R* (121)	49 813.01	−0.02
R (46)	48 535.00*	−0.22	*R* (122)	49 817.01	0.03
R (62)	48 965.83	0.01	*R* (123)	49 820.56	−0.01
R (67)	49 083.05*	−0.21	*R* (124)	49 823.84	0.04
R (68)	49 105.77	0.01	*R* (125)	49 826.72	0.04
R (69)	49 127.88	−0.05	*R* (127)	49 831.38	0.02
R (70)	49 149.92*	0.16	*R* (128)	49 833.19	0.03
R (86)	49 453.71	−0.02	*R* (129)	49 834.61	0.01
R (87)	49 469.92	0.06	*R* (130)	49 835.71	0.04
R (88)	49 485.66	0	*R* (131)	49 836.42	0.03
R (89)	49 501.09	−0.02	*R* (132)	49 836.79	0.04
R (90)	49 516.28	0.06	*R* (147)	49 798.47	0.11
R (91)	49 531.06	0.06			

$^{205}Tl^{19}F$ $v' = 3 \leftarrow v'' = 2$					
Line	$\tilde{\nu}/m^{-1}$	$\delta\tilde{\nu}/m^{-1}$	Line	$\tilde{\nu}/m^{-1}$	$\delta\tilde{\nu}/m^{-1}$
P (30)	44 919.24	0.02	*R* (54)	48 305.93	0.02
R (33)	47 675.02	0.05	*R* (60)	48 460.20	−0.02
R (34)	47 708.16	−0.02	*R* (63)	48 532.77*	−0.22
R (35)	47 741.19	0.11	*R* (64)	48 556.48*	−0.11
R (42)	47 962.52	−0.01	*R* (84)	48 959.25	0.03
R (45)	48 053.14*	0.45	*R* (85)	48 975.84	−0.01
R (46)	48 082.06	−0.04	*R* (93)	49 096.60	−0.05
R (48)	48 139.94	−0.05	*R* (94)	49 110.08*	−0.14
R (53)	48 279.19*	0.13	*R* (95)	49 123.39	−0.06

$^{205}Tl^{19}F$ $v' = 4 \leftarrow v'' = 3$					
Line	$\tilde{\nu}/m^{-1}$	$\delta\tilde{\nu}/m^{-1}$	Line	$\tilde{\nu}/m^{-1}$	$\delta\tilde{\nu}/m^{-1}$
P (19)	45 047.42	−0.06	*R* (65)	48 125.94	−0.02
P (12)	45 383.16	−0.06	*R* (66)	48 148.75	0.06
R (49)	47 718.07	0	*R* (72)	48 278.34*	0.12
R (50)	47 746.06	0.08	*R* (73)	48 298.74	0.09
R (58)	47 957.69	0.01	*R* (81)	48 450.29	0.09
R (62)	48 056.20*	0.41	*R* (82)	48 467.52*	−0.13
R (63)	48 079.47	−0.03	*R* (87)	48 549.81	−0.03
R (64)	48 102.83	−0.06			

TABLE 1. (*concluded*)

		$^{205}Tl^{19}F$ $v' = 5 \leftarrow v'' = 4$			
Line	$\tilde{\nu}/m^{-1}$	$\delta\tilde{\nu}/m^{-1}$	Line	$\tilde{\nu}/m^{-1}$	$\delta\tilde{\nu}/m^{-1}$
P (2)	45 404.96	−0.04	*R* (79)	47 961.07	−0.02
R (64)	47 652.59	−0.09	*R* (91)	48 154.23	0.13
R (67)	47 720.31	0.05	*R* (102)	48 288.42	0.08
R (68)	47 742.26*	0.12			
		$^{205}Tl^{19}F$ $v' = 6 \leftarrow v'' = 5$			
Line	$\tilde{\nu}/m^{-1}$	$\delta\tilde{\nu}/m^{-1}$	Line	$\tilde{\nu}/m^{-1}$	$\delta\tilde{\nu}/m^{-1}$
R (7)	45 394.99*	0.13	*R* (90)	47 688.23	0.06
R (88)	47 658.89*	−0.14	*R* (91)	47 702.15	−0.08
R (89)	47 673.75	−0.01	*R* (93)	47 729.40	0.05
		$^{205}Tl^{19}F$ $v' = 7 \leftarrow v'' = 6$			
Line	$\tilde{\nu}/m^{-1}$	$\delta\tilde{\nu}/m^{-1}$	Line	$\tilde{\nu}/m^{-1}$	$\delta\tilde{\nu}/m^{-1}$
R (6)	44 925.28	0.06	*R* (18)	45 389.93	0.07
		$^{205}Tl^{19}F$ $v' = 8 \leftarrow v'' = 7$			
Line	$\tilde{\nu}/m^{-1}$	$\delta\tilde{\nu}/m^{-1}$			
R (31)	45 411.97	−0.10			

[a]In Tables 1 and 2, for each designated line of the specified band of a particular isotopic variant, $\tilde{\nu}$ is the measured wave number and $\delta\tilde{\nu}$ is the difference between the wave number measured and wave number calculated with the parameters in Table 3. Asterisks mark lines that were effectively precluded from influencing the fit.

$$V(z) = c_0 z^2\left(1 + \sum_{j=1} c_j z^j\right) \tag{3}$$

For an assumed diatomic molecule AB having nuclei with protons of unequal number, further functions dependent on individual nuclear masses M_a and M_b include those for nonadiabatic vibrational effects [9], whereby electrons imperfectly follow nuclei during oscillations of the latter with respect to the centre of mass,

$$\beta(R) = \beta^a(R) + \beta^b(R) = m_e\left(\sum_{j=0} \frac{s_j^a z^j}{M_a} + \sum_{j=0} \frac{s_j^b z^j}{M_b}\right) \tag{4}$$

for nonadiabatic rotational effects, whereby electrons follow imperfectly nuclei during rotations of the latter about the centre of mass,

$$\alpha(R) = \alpha^a(R) + \alpha^b(R) = m_e\left(\sum_{j=0} \frac{t_j^a z^j}{M_a} + \sum_{j=0} \frac{t_j^b z^j}{M_b}\right) \tag{5}$$

and for the contribution to the internuclear potential energy dependent on nuclear mass, i.e., generally the adiabatic effects whereby the potential energy depends not only on the distance between the nuclei but also slightly on their relative momenta,

$$V'(R) = V^a(R) + V^b(R) = m_e\left(\sum_{j=1} \frac{u_j^a z^j}{M_a} + \sum_{j=1} \frac{u_j^b z^j}{M_b}\right) \tag{6}$$

As nuclear masses are known generally much less accurately than atomic masses and as the discrepancies between these masses have immaterial effects on the ultimate parameters and their interpretation, we employed atomic masses [15].

We express the discrete molecular energies $\tilde{E}_{vJ}$ or vibration–rotational terms, of which the differences $\tilde{\nu} = \tilde{E}_{v'J'} - \tilde{E}_{vJ}$ are the measured wave numbers of transitions, within a particular electronic state, in the form [9]

$$\tilde{E}_{vJ} = \sum_{k=0}\sum_{l=0} (Y_{kl} + Z_{kl}^{r,a} + Z_{kl}^{r,b} + Z_{kl}^{v,a} + Z_{kl}^{v,b}) \times \left(v + \frac{1}{2}\right)^k [J(J+1)]^l \tag{7}$$

The dependence of the term coefficients Y_{kl} and Z_{kl} on the equilibrium internuclear separation R_e, the equilibrium force coefficient k_e, and the coefficients in the radial functions defined in (3)–(6) is explained elsewhere [9]. In (7), which defines the eigenvalues of the Hamiltonian in (1), the explicit dependences of E_{vJ}, Y_{kl}, and various Z_{kl} on the isotopic varriant are suppressed. To treat adiabatic and nonadiabatic effects, which imply the coupling of electronic and nuclear motions, by means of radial functions of R, which imply the separate treatment of these

TABLE 2. Assignments of vibration–rotational transitions of $^{203}Tl^{19}F$ measured with a diode laser[a]

$^{203}Tl^{19}F$ $v' = 1 \leftarrow v'' = 0$					
Line	$\tilde{\nu}/m^{-1}$	$\delta\tilde{\nu}/m^{-1}$	Line	$\tilde{\nu}/m^{-1}$	$\delta\tilde{\nu}/m^{-1}$
P (46)	44 916.19	−0.06	*R* (50)	49 129.04	−0.06
P (44)	45 030.98	−0.04	*R* (62)	49 447.07	−0.11
R (8)	47 653.84	−0.03	*R* (63)	49 471.56	0
R (9)	47 695.27	−0.10	*R* (64)	49 495.60	0
R (10)	47 736.67	0.11	*R* (65)	49 519.27	−0.05
R (18)	48 055.64*	0.56	*R* (66)	49 542.61	−0.09
R (19)	48 093.49	−0.02	*R* (77)	49 777.83	−0.12
R (20)	48 131.60	−0.03	*R* (78)	49 797.32	0
R (24)	48 281.12	0.11	*R* (79)	49 816.31	−0.05
R (29)	48 460.67	−0.05	*R* (80)	49 835.09	0.03
R (31)	49 530.56	0.15	*R* (81)	49 853.42	0
R (45)	48 982.70	−0.05	*R* (82)	49 871.44	0
R (49)	49 100.46	−0.02			

$^{203}Tl^{19}F$ $v' = 2 \leftarrow v'' = 1$					
Line	$\tilde{\nu}/m^{-1}$	$\delta\tilde{\nu}/m^{-1}$	Line	$\tilde{\nu}/m^{-1}$	$\delta\tilde{\nu}/m^{-1}$
P (36)	45 046.10	−0.10	*R* (113)	49 789.36	−0.03
R (20)	47 681.16*	−0.18	*R* (114)	49 796.12	−0.05
R (21)	47 718.85	−0.03	*R* (115)	49 802.59	0
R (31)	48 077.12	−0.08	*R* (116)	49 808.47*	−0.19
R (33)	48 145.12	0.01	*R* (117)	49 814.35	−0.02
R (37)	48 277.23	0.07	*R* (118)	49 819.72	−0.01
R (38)	48 309.41	0.03	*R* (119)	49 824.75	0.01
R (43)	48 465.62	−0.11	*R* (120)	49 829.31	−0.07
R (46)	48 555.50*	−0.21	*R* (121)	49 833.67	−0.01
R (66)	49 080.99*	−0.22	*R* (122)	49 837.64	0.03
R (67)	49 103.98	−0.07	*R* (123)	49 841.17	−0.02
R (68)	49 126.61	0.05	*R* (124)	49 844.43	0.02
R (69)	49 148.86	0.13	*R* (125)	49 847.28	0.01
R (85)	49 458.11	−0.03	*R* (127)	49 851.91	0
R (87)	49 490.77	0.02	*R* (130)	49 856.14	−0.03
R (88)	49 506.50	−0.05	*R* (131)	49 856.88	0.01
R (89)	49 522.13	0.13	*R* (132)	49 857.21	0
R (91)	49 551.90	0.02	*R* (140)	49 846.79	−0.01
R (111)	49 774.75	−0.03	*R* (141)	49 843.92	0.06
R (112)	49 782.20	−0.06	*R* (142)	49 840.61	0.06

$^{203}Tl^{19}F$ $v' = 3 \leftarrow v'' = 2$					
Line	$\tilde{\nu}/m^{-1}$	$\delta\tilde{\nu}/m^{-1}$	Line	$\tilde{\nu}/m^{-1}$	$\delta\tilde{\nu}/m^{-1}$
P (28)	45 041.14	−0.07	*R* (52)	48 272.10	−0.01
P (21)	45 397.42*	−0.18	*R* (53)	48 299.35	0.06
R (32)	47 661.26	−0.02	*R* (59)	48 455.60	−0.03
R (33)	47 694.68	−0.14	*R* (63)	48 553.20	−0.15
R (34)	47 728.06	0	*R* (83)	48 962.73	−0.03
R (41)	47 951.82	−0.04	*R* (92)	49 103.17	−0.07
R (45)	48 072.61	−0.18	*R* (94)	49 130.68	−0.03
R (46)	48 102.11	−0.11	*R* (95)	49 144.03	0.10
R (47)	48 131.23	−0.11			

$^{203}Tl^{19}F$ $v' = 4 \leftarrow v'' = 3$					
Line	$\tilde{\nu}/m^{-1}$	$\delta\tilde{\nu}/m^{-1}$	Line	$\tilde{\nu}/m^{-1}$	$\delta\tilde{\nu}/m^{-1}$
P (22)	44 916.80	−0.08	*R* (62)	48 075.68	−0.08
P (19)	45 065.16	−0.05	*R* (64)	48 122.79	−0.10
P (12)	45 401.14	−0.11	*R* (65)	48 146.00	0.04
R (46)	47 652.06	−0.13	*R* (71)	48 277.60	0.09
R (47)	47 680.88*	−0.19	*R* (72)	48 298.30	0.02
R (48)	47 709.54	−0.09	*R* (80)	48 452.52	−0.01
R (49)	47 737.95	0.08	*R* (81)	48 470.21	−0.10
R (57)	47 952.22	−0.04			

TABLE 2. (*concluded*)

$^{203}Tl^{19}F$ $v' = 5 \leftarrow v'' = 4$					
Line	$\tilde{\nu}/m^{-1}$	$\delta\tilde{\nu}/m^{-1}$	Line	$\tilde{\nu}/m^{-1}$	$\delta\tilde{\nu}/m^{-1}$
P (13)	44 923.91	−0.04	*R* (66)	47 717.59	−0.11
P (10)	45 063.52	−0.03	*R* (67)	47 739.98	0.07
R (63)	47 649 06	−0.05	*R* (88)	48 130.03	−0.08
R (64)	47 672.32	0.02			

$^{203}Tl^{19}F$ $v' = 6 \leftarrow v'' = 5$					
Line	$\tilde{\nu}/m^{-1}$	$\delta\tilde{\nu}/m^{-1}$	Line	$\tilde{\nu}/m^{-1}$	$\delta\tilde{\nu}/m^{-1}$
R (7)	45 412.70	−0.20	*R* (87)	47 663.24	−0.07
R (86)	47 647.78	−0.13	*R* (88)	47 678.13	−0.25

$^{203}Tl^{19}F$ $v' = 7 \leftarrow v'' = 6$					
Line	$\tilde{\nu}/m^{-1}$	$\delta\tilde{\nu}/m^{-1}$	Line	$\tilde{\nu}/m^{-1}$	$\delta\tilde{\nu}/m^{-1}$
R (18)	45 407.84	−0.03			

[a]Read the footnote of Table 1.

motions, may appear incongruous; for the electronic ground state and in particular for its vibration–rotational states far from the dissociation limit, the formal interactions with energetically distant, electronically excited states may, however, be sufficiently weak that they can be considered to represent small and homogeneous perturbations [11].

Even though these adiabatic and nonadiabatic effects are mathematical artifacts, for the reason just stated, experimental information is associated specifically with the nonadiabatic rotational effects. The rotation of an otherwise nonmagnetic diatomic molecule induces a small magnetic dipolar moment [16]; the interaction of this molecular moment with an externally applied magnetic field produces splitting of spectral lines according to the Zeeman effect. The rotational *g* factor, or g_J, which is proportional to the magnetogyric ratio, the quotient of the induced rotational magnetic dipolar moment and the rotational angular momentum, is a measure of the extent of the splitting, according to M_J, of the energy of a particular vibration–rotational state (for $J > 0$). The factor g_J is thus an expectation value $\langle vJ|\alpha(R)|vJ\rangle$ or $\langle vJ|g_J(R)|vJ\rangle$ of a particular state denoted by vibrational quantum number v and rotational quantum number J. For a net electrically neutral diatomic molecule of relative electric polarity $^{+}AB^{-}$, there arise two contributions to the *g* factor, one, g_J^{na}, attributed to interaction between electronic and nuclear motions and the other from a rotating electric dipolar moment μ_e (at the equilibrium internuclear distance R_e) [17]:

$$g_J = g_J^{na} + m_p(M_a^{-1} - M_b^{-1})\frac{\mu_e}{(eR_e)} \tag{8}$$

in which m_p is the mass of the proton and e its electric charge. The equations, adapted from ref. 18, for partition of the *g* factor to contributions of the separate atomic centres thus become

$$t_0^a = \mu\left(\frac{g_J}{m_p} + \frac{2\mu_e}{eR_eM_b}\right) \tag{9}$$

$$t_0^b = \mu\left(\frac{g_J}{m_p} - \frac{2\mu_e}{eR_eM_a}\right) \tag{10}$$

There are radial functions of three kinds beyond mechanical effects embodied in the potential energy $V(z)$ [9], namely functions for adiabatic, nondiabatic rotational, and nonadiabatic vibrational effects of atomic centres of each type; in practice, information of at most two kinds can generally be deduced from spectra recorded for samples without externally applied fields, namely the dependence on individual atomic (or nuclear) masses and the extra rotational effects. Measurements of the rotational *g* factor in varied vibration–rotational states by means of the Zeeman effect provide information that enables, in principle, separate evaluation of nonadiabatic rotational effects [9].

4. Application of theory to spectra of TlF

On the basis of an analysis of all pure rotational spectral transitions of TlF [2–6] and the vibration–rotational spectra recorded under moderate resolution [8], we predicted the wave numbers of vibration–rotational transitions in bands of the sequence $\Delta v = 1$ of both $^{205}Tl\,^{19}F$ and $^{203}Tl^{19}F$ within the range of measurements with laser diodes. Because of the quality of the former spectra and their assignments [8], the differences between these predicted wave numbers and those newly measured were small, enabling assignment of the lines in bands of progressively greater v. Following these assignments of bands with small values of v, we incorporated these lines into the fitting programme and extended predictions to $v = 10$. By means of this iterative process we fitted successfully most measured lines within the range $44\,900 \leq \tilde{\nu}/m^{-1} \leq 50\,000$; the assignments appear in Tables 1 and 2. With differences of spectral terms each weighted appropriately as input, we fit by means of the programme RADIATOM [9] the coefficients of the radial functions within the analytic expression of the term coefficients Y_{kl} and the various Z_{kl} directly, according to (7); after various trial sets, parameters evaluated in the most significant set according to the criterion of the *F* value [9] are presented in Table 3.

To ensure the maximum physical significance of all primary parameters evaluated by means of RADIATOM, during the fit we imposed the values $t_0^{Tl} = -0.158\,07 \pm 0.000\,17$ and $t_0^{F} = -0.995\,81 \pm 0.000\,98$ derived from the measured molecular rotational *g* factor, $g_J = -0.053\,56 \pm 0.000\,05$ [7],

TABLE 3. Coefficients of radial functions and other molecular properties of TlF and InF, all independent of nuclear mass; M = Tl or In[a]

Parameter	Values	
	TlF $X0^+$	InF $X0^+$
c_0/m^{-1}	25 482 480.6 ± 67	27 314 096.9 ± 16.4
c_1	−2.400 110 ± 0.000 036	−2.437 213 ± 0.000 027
c_2	3.394 578 ± 0.000 24	−3.570 881 ± 0.000 24
c_3	−3.397 89 ± 0.004 6	−3.512 32 ± 0.003 6
c_4	2.330 7 ± 0.043	1.715 6 ± 0.036
c_5	1.012 3 ± 0.103	0.522 5 ± 0.187
c_6	[0]	6.049 ± 1.19
t_0^{M}	[−0.158 07]	[−0.287]
t_0^{F}	[−0.995 81]	[−1.00]
$u_1^{\mathrm{M}}/10^6\ \mathrm{m}^{-1}$	−508.79 ± 31.4	[0]
$U_{1,0}/\mathrm{m}^{-1}\ \mathrm{u}^{1/2}$	198 874.053 ± 0.067	216 162.735 ± 0.072
$U_{0,1}/\mathrm{m}^{-1}\ \mathrm{u}$	388.020 40 ± 0.001 29	427.675 938 ± 0.000 030
$k_e/\mathrm{N\ m}^{-1}$	233.027 29 ± 0.000 21	275.303 79 ± 0.000 25
$R_e/10^{-10}\ \mathrm{m}$	2.084 351 7 ± 0.000 003 9	1.985 367 3 ± 0.000 001 67
	$^{205}\mathrm{Tl}^{19}\mathrm{F}$	$^{115}\mathrm{In}^{19}\mathrm{F}$
ω_e/m^{-1}	47 694.401 7 ± 0.016 1	53 536.369 9 ± 0.017 9
B_e/m^{-1}	22.316 862 ± 0.000 074	26.233 183 9 ± 0.000 001 8

[a]Each specified uncertainty denotes one estimated standard error propagated from input data of frequencies and wave numbers; errors of k_e and R_e include uncertainties of fundamental constants h and N_a; brackets enclose values, of which estimated standard errors are discussed in the text, that were constrained during fits of input spectral data.

and the known electric dipolar moment, $\mu_e = (1.398\ 83 \pm 0.000\ 27) \times 10^{-29}$ C m [7], according to (9) and (10) for assumed $^+\mathrm{TlF}^-$. Values of neither other $t_J^{\mathrm{Tl,F}}$ nor any $s_J^{\mathrm{Tl,F}}$ were evaluated. Because the values of $t_0^{\mathrm{Tl,F}}$ are highly precise and because they occur in only the correction terms Z_{kl}^r, their uncertainty has a negligible influence on uncertainties of other parameters. Hence only seven independently adjustable parameters of the potential-energy function, namely R_e and c_j with $0 \leq j \leq 5$, with one value of the coefficient u_1^{Tl}, suffice to represent the 1079 transitions essentially within the uncertainty of experimental measurements. The latter consisted of 89 assorted pure rotational lines [2–6], 760 vibration–rotational lines measured in emission [8], and 230 vibration–rotational lines newly measured in absorption; many lines of the latter group duplicated corresponding transitions of the large group measured in emission. Because the uncertainties of pure rotational transitions had evidently been estimated conservatively if the microwave frequencies specified by the original authors were accompanied by estimated single standard errors, we used half the reported values of the uncertainties [2–6], which still yielded an excellent fit of these data. With uncertainties of most vibration–rotational lines of $^{205}\mathrm{Tl}^{19}\mathrm{F}$ measured in absorption set at 0.035 m^{-1}, and lines of $^{203}\mathrm{Tl}^{19}\mathrm{F}$ and all vibration–rotational transitions measured in emission at larger values appropriate to the relative abundance of the isotopic variants of Tl and to the effective spectral resolution of the measurements [8], the reduced standard deviation of the fit was $\sigma = 1.28$ and the F value [9] was 4.3×10^{14}. In the nonlinear fitting process the weights of all pure rotational and vibration–rotational transitions were the reciprocal squares of assigned uncertainties. The estimated single standard errors accompanying values of parameters in Table 3 reflect collective propagation of error of measurement of the various frequencies and wave numbers; the error in k_e and R_e takes into account also uncertainties of fundamental constants h and N_A [20]. All parameters of TlF presented in Table 3 have satisfactorily large values of the ratio of the magnitude of each parameter to its estimated standard error. The maximum range of validity of the radial functions of TlF is $1.85 \leq R/10^{-10}\ \mathrm{m} \leq 2.45$.

The programme RADIATOM yielded secondarily parameters U_{kl} and nonmechanical contributions to $\Delta_{kl}^{\mathrm{Tl,F}}$ in an empirical relation [19]

$$\tilde{E}_{vJ} = \sum_{k=0} \sum_{l=0} U_{kl} \mu^{(-(k/2)+1)} \left(v + \frac{1}{2}\right)^k [J(J+1)]^l \times \left[1 + m_e\left(\frac{\Delta_{kl}^{\mathrm{Tl}}}{M_{\mathrm{Tl}}} + \frac{\Delta_{kl}^{\mathrm{F}}}{M_{\mathrm{F}}}\right)\right] \quad (11)$$

in which the coefficients U_{kl} are related to only the parameters R_e and coefficients c_j, $j \geq 0$, whereas coefficients $\Delta_{kl}^{\mathrm{Tl,F}}$ are formally independent of mass. This equation serves to define both the auxiliary parameters $U_{1,0}$ and $U_{0,1}$ that appear in Table 3 and the quantities Δ_{kl} for comparison with previous work.

5. Discussion

With only eight adjustable parameters and two constrained coefficients (t_0^{Tl} and t_0^{F}) derived from separate experiments (Stark and Zeeman effects), we succeeded in reproducing the frequencies of 89 pure rotational transitions and the wave numbers of about 800 distinct vibration–rotational transitions of both $^{205}\mathrm{Tl}^{19}\mathrm{F}$ and $^{203}\mathrm{Tl}^{19}\mathrm{F}$ almost within the uncertainties of their

measurements; for the lines newly measured with diode lasers the relative precision of the measurements was about $\delta\tilde{\nu}/\tilde{\nu} \sim 10^{-6}$. That the reduced standard deviation of the fit slightly exceeded unity likely indicates that uncertainties assigned to wave numbers of the latter lines in absorption were slight underestimates, because a separate weighted fit of only microwave transitions and infrared lines in emission yielded a reduced standard deviation near 1.0. Because lines in infrared absorption duplicated some emission transitions, the smaller uncertainties ensured emphasis on the new measurements having increased precision. When we added a further variable u_2^{Tl} to the parameter set, the fit converged, and the systematic but slight deviations in the 6–5 band of ^{203}Tl^{19}F significantly decreased; however, this parameter was evaluated with only marginal significance ($\delta u_2^{\mathrm{Tl}}/u_2^{\mathrm{Tl}} \sim 0.45$) and the F statistic became smaller than in its absence, and likewise for other tested models. For this reason the parameters in Table 3 represent the optimum set in terms of the specified radial functions. In Tables 1 and 2 and residuals of individual lines resulting from the fit indicate the quality of measurements and their representation according to only 10 independent parameters (c_0–c_5, R_e, u_1^{Tl}, and t_0^{Tl} and t_0^{F} or g_J and μ_e). To reproduce or to extend transition frequencies, one readily substitutes these parameters into simple analytic expressions [9, 21] to form term coefficients Y_{kl} and Z_{kl} of eigenvalues according to (7).

Other than parameters defining the potential-energy function or equivalent quantities ($U_{1,0}$ and $U_{0,1}$), only three parameters of TlF appear in Table 3: the values of t_0^{Tl} and t_0^{F} imposed on the basis of the molecular rotational g factor and μ_e, and the further coefficient u_1^{Tl}. That the latter quantity has an atypically large magnitude is confirmed, with reference to (11), by the value $\Delta_{0,1}^{\mathrm{Tl}} = -20.13 \pm 1.24$; in other molecules $\Delta_{0,1}$ and $\Delta_{1,0}$ have magnitudes typically of the order of unity, and the value $\Delta_{0,1}^{\mathrm{F}} = -0.9958 \pm 0.0001$ has indeed the expected magnitude. Analysis of contributions to $\Delta_{0,1}^{\mathrm{Tl}}$, from which purely mechanical contributions were excluded, indicates a rotational component -0.158 from $Z_{0,1}^{r,\mathrm{Tl}}$ and a vibrational component -19.966 from $Z_{0,1}^{v,\mathrm{Tl}}$, according to (7). Both the value of $\Delta_{0,1}^{\mathrm{F}}$ and the rotational contribution to $\Delta_{0,1}^{\mathrm{Tl}}$ reflect exactly the values of $t_0^{\mathrm{Tl,F}}$ generated from g_J. Although the vibrational component or u_1^{Tl} is generally related to adiabatic effects [9], we have no particular reason to associate such an extraordinarily large adiabatic effect with a nucleus so relatively massive as Tl, as results of analysis of spectra of other, less massive, molecules such as SiS [22] directly verify.

To explore the basis of the large magnitude we undertook comparison with the related molecule InF, nominally isovalent: In is located just above Tl in the periodic table within group 13. Infrared spectra of InF in absorption were measured previously [23] with diode lasers. We applied the programme RADIATOM [9] to 8 rotational transitions in the microwave region [4], a further set of 11 pure rotational transitions in the millimetre-wave region [24], and 636 vibration–rotational transitions of ^{115}In^{19}F and ^{113}In^{19}F [23]; our set of 655 data included these many vibration–rotational transitions measured in absorption at high resolution [23], but not emission spectra at low resolution [25]. To facilitate comparison with results on TlF, we sought to impose values of $t_0^{\mathrm{In,F}}$ generated from an experimental value of g_J, but no such value is available. We observed that values of t_0^{F} of AlF, GaF, and TlF are, respectively, -1.05, -1.013, and -0.9958. Hence we expect that t_0^{F} of $^{+}$InF^{-} is correspondingly -1.00 ± 0.01; with both this assumption and the known electric dipolar moment $\mu_e = (1.134 \pm 0.011) \times 10^{-29}$ C m of InF [4], we estimate $g_J = -0.0555 \pm 0.0005$ according to (10) and $t_0^{\mathrm{In}} = -0.287 \pm 0.005$ according to (9). With these values of $t_0^{\mathrm{In,F}}$ applied as constraints, we derived values of c_j, $0 \leq j \leq 6$, and other molecular properties of InF listed in Table 3. We imposed as uncertainties of wave numbers of the corresponding lines in the collected data the standard deviations of fits of individual bands of ^{115}In^{19}F and ^{113}In^{19}F, taking half the conservatively reported uncertainties of microwave frequencies [24] as for TlF. For InF previous analysis [23] yielded no value of an inverse mass coefficient $\Delta_{kl}^{\mathrm{In}}$. Testing for the utility of u_1^{In}, we found that although a value was marginally significant, as $\delta u_1^{\mathrm{In}}/|u_1^{\mathrm{In}}| \sim 0.5$, there was strong correlation between u_1^{In} and $U_{0,1}$, and the error in R_e became exceptionally large; in the final fit we therefore discarded u_1^{In} from the set of adjustable parameters, which yielded a significantly enhanced value of the F statistic. We concluded that the magnitude of u_1^{In} is relatively small. That the reduced standard deviation of the fit is 1.009 and that the F value is 1.124×10^{14} both indicate a satisfactory fit. Of the potential-energy function of InF in Table 3 the maximum range of validity is $1.76 \leq R/10^{-10}\,\mathrm{m} \leq 2.35$.

Comparing the results for TlF and InF in Table 3, we discern that the values of some corresponding parameters are similar, for instance the values of c_1, c_2, and c_3, whereas values of c_0 and k_e of TlF are smaller than those of InF, as expected in proceeding down a group of the periodic table, and R_e of TlF is analogously larger than R_e of InF. For TlF, inclusion of c_6 was unnecessary, consistent with the poorly defined value of $Y_{4,0}$ from analysis of the emission spectra [8]. In contrast, for InF c_6 is absolutely required, as without this parameter the best fit had a reduced standard deviation about 3.6. For neither TlF nor InF could we define values of s_j related to nonadiabatic vibrational effects.

Returning to the anomalously large magnitude of u_1^{Tl}, we recall that such large, apparently adiabatic, effects were detected previously for diatomic compounds of both Tl and Pb, but not of In [26]. The "adiabatic" value $\Delta_{0,1}^{\mathrm{Tl}} = -18.6 \pm 1.1$ [26] agrees satisfactorily with, and is confirmed by, our vibrational contribution -20.0 ± 1.2 based on more extensive data, and the "nonadiabatic" (actually the nonadiabatic rotational) value $\Delta_{0,1}^{\mathrm{Tl}} = -0.152$ [26] is expected to be identical to our value $t_0^{\mathrm{Tl}} = -0.158$. The adiabatic value $\Delta_{0,1}^{\mathrm{In}}$ of InI was only -2.37 ± 0.45 [26]. These adiabatic effects of compounds of Tl and Pb were subsequently reinterpreted to reflect not the effect of finite masses of isotopic variants but their nuclear volumes [27]: just as adiabatic and purely nonadiabatic effects vanish in the limit of infinitely massive nuclei, so the isotopic field shift vanishes in the limit of nil nuclear volume. Hence the present results on TlF are consistent with the finite and isotopically varying volume of nuclei of Tl having a detectable effect on spectral terms and transition wave numbers in vibration–rotational spectra; the same effect was only marginally evaluated for In in InI [28]. As our value of the vibrational contribution to $\Delta_{0,1}^{\mathrm{Tl}}$ essentially reproduces, and confirms independently according to our separate calculation, the earlier value obtained from data of only pure rotational transitions [27], elaboration of this phenomenon is here superfluous. Because a large magnitude of u_1^{In} from our analysis of spectra of InF or an anomalously large magnitude of $\Delta_{0,1}^{\mathrm{In}}$ is lacking, we detect no effect of a significant variation of nuclear volume between ^{113}In and ^{115}In.

Of the contributions to the molecular rotational g factor of TlF, the electric dipolar moment contributes $-0.047\,75$ according to

(8), corresponding to 90% of the measured value of g_J. For InF the known electric dipolar moment contributes −0.0439 36 to g_J, thus accounting for 80% of the value expected according to our prediction. According to Table 3, all the purely adiabatic and nonadiabatic effects are relatively small for these massive molecules; the parameters additional to those for the potential-energy function for both TlF and InF are aptly attributed mostly to effects of a distorted distribution of electronic mass associated with the strongly dipolar distribution of electronic charge, relative to noninteracting neutral atoms, and for TlF also to a finite and isotopically varying nuclear volume of Tl rather than to finite nuclear mass.

6. Conclusion

We analysed vibration–rotational spectra of TlF measured in absorption from diode lasers as sources, which we combined with other data of transition frequencies and wave numbers. We express the results in the form of radial functions [9] that constitute the most compact and physically meaningful representation. The parameters include u_1^{Tl}, which has a negative sign and an atypically large magnitude (unlike u_1^{In}, which was not evaluated significantly), and which we relate to the effect of a finite and isotopically variable nuclear volume of Tl on rotational terms of its isotopic molecules [27], rather than to adiabatic effects characteristic of less massive nuclei [9]. Because this interpretation of u_1^{Tl} does not conform to adiabatic effects [9], u_1^{Tl} is thus an effective parameter applicable rigorously only to ^{203}Tl and ^{205}Tl. Nevertheless, these parameters in Table 3 still represent the most compact and meaningful representation of the available pure rotational and vibration–rotational spectral data of TlF; one can thereby reproduce by means of simple analytic expressions [9, 21] these data essentially within the accuracy of their measurements.

Acknowledgments

We thank Dr. J.W.C. Johns for providing spectral data of SO_2 for purposes of calibration and Dr. Yasushi Ozaki for providing a file of spectral transitions of InF [23]. J.F.O. and S.C.L. thank the National Science Council of the Republic of China for research support.

1. G. Herzberg. Molecular spectra and molecular structure. I. Spectra of diatomic molecules. 2nd ed. Van Nostrand, New York. 1950.
2. A.H. Barrett and M. Mandel. Phys. Rev. **109**, 1572 (1958).
3. H.G. Fitzky. Z. Phys. **151**, 351 (1958).
4. J. Hoeft, F.J. Lovas, E. Tiemann, and T. Torring. Z. Naturforsch. A: Astrophys. Phys. Phys. Chem. **25**, 1029 (1970).
5. K.P.R. Nair and J. Hoeft. Chem. Phys. Lett. **96**, 348 (1983).
6. J. Hoeft and K.P.R. Nair. Z. Phys. D: At. Mol. Clusters, **5**, 345 (1987).
7. R. von Boeckh, C. Graff, and R. Ley. Z. Phys. **179**, 285 (1964).
8. H. Uehara, K. Horiai, A. Kerim, and N. Aota. Chem. Phys. Lett. **189**, 217 (1992).
9. J.F. Ogilvie. J. Phys. B: At. Mol. Opt. Phys. **27**, 47 (1994).
10. J.F. Ogilvie and S.F. Chuang. J. Mol. Spectrosc. **156**, 1 (1992).
11. F.M. Fernandez and J.F. Ogilvie. Chin. J. Phys. **30**, 177 (1992); **30**, 599 (1992), and references therein.
12. J.F. Ogilvie. Proc. R. Soc. London, A: **378**, 287 (1981); **381**, 479 (1982).
13. J.F. Ogilvie. J. Chem. Phys. **88**, 2804 (1988).
14. E.R. Cohen and P. Giacomo. Physica A (Amsterdam), **146**, 1 (1987).
15. A.H. Wapstra and G. Audi. Nucl. Phys. **A432**, 1 (1985).
16. W. Gordy and R.L. Cook. Microwave molecular spectra. Wiley, New York. 1984.
17. E. Tiemann and J.F. Ogilvie. J. Mol. Spectrosc. **165**, 377 (1994).
18. E. Tiemann, W.U. Stieda, T. Torring, and J. Hoeft. Z. Naturforsch. A: Phys. Phys. Chem. Kosmophys. **30**, 1606 (1975).
19. A.H.M. Ross, R.S. Eng, and H. Kildal. Opt. Commun. **12**, 433 (1974).
20. E.R. Cohen and B.N. Taylor. Rev. Mod. Phys. **59**, 1121 (1987).
21. J.F. Ogilvie. Comput. Phys. Commun. **30**, 101 (1983).
22. J.F. Ogilvie and S.-C. Liao. Acta Phys. Hung. **74**, 355 (1994).
23. Y. Ozaki, K. Horiai, K. Nakagawa, and H. Uehara. J. Mol. Spectrosc. **158**, 363 (1993).
24. J. Hoeft and K.P.R. Nair. Z. Phys. D: At. Mol. Clusters, **162**, 203 (1994).
25. H. Uehara, K. Horiai, T. Mitani, and H. Suguro. Chem. Phys. Lett. **162**, 137 (1989).
26. E. Tiemann, H. Arnst, W.U. Stieda, T. Torring, and J. Hoeft. Chem. Phys. **67**, 133 (1982).
27. J. Schlembach and E. Tiemann. Chem. Phys. **68**, 21 (1982).